Journal of the Korean Society of Marine Engineering, Vol. 39, No. 8 pp. 856~862, 2015
J. Korean Soc. of Marine Engineering (JKOSME)
http://dx.doi.org/10.5916/jkosme.2015.39.8.856

ISSN 2234-7925 (Print)
ISSN 2234-8352 (Online)
**Original Paper**

# Hydrofoil selection and design of a 50W class horizontal axis tidal current turbine model

Seung-Jun Kim[1]· Patrick Mark Singh[2]· Young-Do Choi†

(Received July 3, 2015 ; Revised September 2, 2015 ; Accepted September 20, 2015)

**Abstract:** Tidal current energy is an important alternative energy resource among the various ocean energy resources available. The tidal currents in the South-Western sea of Korea can be utilized for the development of tidal current power generation. Tidal power generation can be beneficial for many fishing nurseries and nearby islands in the southwest region of Korea. Moreover, tidal power generation is necessary for promoting energy self-sufficient islands. As tidal currents are always available, power generation is predictable; thus, tidal power is a reliable renewable energy resource. The selection of an appropriate hydrofoil is important for designing a tidal current turbine. This study concentrates on the selection and numerical analysis of four different hydrofoils (MNU26, NACA63421, DU91_W2_250, and DU93_W_210LM). Blade element momentum theory is used for configuring the design of a 50 W class turbine rotor blade. The optimized blade geometry is used for computational fluid dynamics (CFD) analysis with hexahedral numerical grids. Among the four blades, NACA63421 blade showed the maximum power coefficient of 0.45 at a tip speed ratio of 6. CFD analysis is used to investigate the power coefficient, pressure coefficient, and streamline distribution of a 50 W class horizontal axis tidal current turbine for different hydrofoils.

**Keywords:** Horizontal axis tidal current turbine, Hydrofoil, Blade element momentum theory, Power coefficient

## 1. Introduction

Among the various ocean energy resources available, tidal current energy is an important alternative energy resource **[1]**. Tidal currents are reliable and predictable **[2]**; thus, it overcomes one of the major limitations of several natural resources, which is the lack of predictability. This lack of predictability leads to periods where little or no energy is generated. In addition, tidal turbines have the potential of minimizing both visual and noise pollution **[3]**.

There are more than one thousand islands located in the southern region of Korea. The local government plans to develop the region for the local people, boost the tourism industry, and build facilities for the processing of marine products **[4]**. The increasing development in this region has led to the demand for cleaner energy resources and minimizing the utilization of diesel power plants. The introduction of tidal power generation will benefit many fishing nurseries and the entire region. Furthermore, tidal power generation can contribute toward promoting energy self-sufficient islands.

Small floating-bridge type tidal current turbines can be installed in the limited space between small islands, instead of large tidal current turbines. The small tidal current turbines can be connected by bridge-type connection in order to increase the output energy, and this energy can be supplied directly to nearby islands in the region. **Figure 1** shows a schematic view of the proposed floating-type tidal current turbine. The floating-type tidal current turbine can be easily accessed for installation and maintenance.

In this study, while developing a floating-bridge type 15kW class small horizontal axis tidal current turbine, as part of the research for the selection and the reduced model test of hydrofoil, a 50 W class horizontal axis tidal current turbine model design is being studied. Blade design was carried out by using four different hydrofoils (MNU26, NACA63421, DU91_W2_250, DU93_W_210LM) to select the appropriate hydrofoil. Blade element momentum theory was used to configure the design of a 50 W turbine rotor blade **[5]**. The goal of this study is to compare results through computational fluid dynamics (CFD) analysis. CFD analysis was conducted to investigate the power coefficient, pressure coefficient, and streamline distribution.

† Corresponding Author (ORCID: http://orcid.org/0000-0001-7316-1153): Department of Mechanical Engineering, Institute of New and Renewable Energy Technology Research, Mokpo National University, (61 Dorim-ri) 1666 Youngsan-Ro, Cheonggye-Myeon, Muan-Gun, Jeonnam, 58555, Korea, E-mail: ydchoi@mokpo.ac.kr, Tel: 061-450-2419
1 Department of Mechanical Engineering, Mokpo National University, E-mail: kimsj617@naver.com, Tel: 061-450-2419
2 Department of Mechanical Engineering, Mokpo National University, E-mail: pms72006@yahoo.com, Tel: 061-450-2419

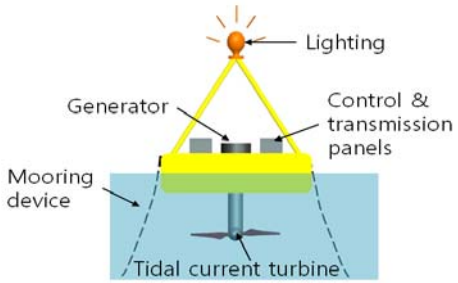


**Figure 1:** Schematic view of proposed floating type tidal current turbine

## 2. Site selection

Tidal current energy is an environmentally friendly energy resource and can be extracted by installing tidal current turbines at the site. Large tidal current energy is available in the south-western coast of Korea. **Figure 2** shows a few high energy density regions where tidal current power plants can be installed. Byun *et al.* **[6]** carried out a study to estimate prospective tidal current energy resources off the south and west coasts of Korea. The study found that the greatest concentration of high energy density regions are located in the Jeonnam Province in the coastal region; the annual energy density can be calculated from **Table 1** as follows 23 MWh·m$^{-2}$ at Uldolmok, 15 MWh·m$^{-2}$ at Maenggol Sudo, 9.2 MWh·m$^{-2}$ at Geocha Sudo and 8.8 MWh·m$^{-2}$ at Jangjuk Sudo.

Tidal power generation is possible at a flow rate of 1 m/s. However, the economical flow rate is approximately 2 m/s. Tidal current is strong in regions located between land and island; these regions are called narrow channels.


**Figure 2:** High energy density regions in Jeonnam Province

**Table 1**: Tidal power candidate locations[4]

| waterway | Max current speed [m/s] | Area [m$^2$] | Annual energy [GWh] |
|---|---|---|---|
| Uldolmok | 4.12 | 8,225 | 182 |
| Jangjuk | 2.25 | 257,300 | 1,014 |
| Geocha | 2.12 | 40,000 | 151 |
| Maenggol | 2.06 | 195,650 | 697 |

By investigating the high energy density regions in Jeonnam province, it is observed that large-scale tidal power generation is possible at Uldolmok, Maenggol channel, and Jangjuk channel. A flow rate of 2 m/s is observed in many regions located between islands and the ends of islands in the south-western coast of Korea.

The purpose of site selection is to design a small 15 kW class tidal current turbine having a flow rate of 2 m/s. Bridge-type 15 kW class small tidal current turbine can be installed in the narrow water channels between the islands located in the Wando region in the south western coast of Korea to generate power for the region. Furthermore, this tidal power generation can be utilized by places that are currently not connected to the national power grid. Moreover, tidal power generation can be utilized as a power source for micro grid systems. However, this study will only focus on a miniature scale 50 W class horizontal axis tidal current turbine (HATCT) of 50 W class.

## 3. Design of 50W class Tidal Current Turbine Rotor Blade

### 3.1 Selection of 50W class Rotor Blade Hydrofoil

Four hydrofoils were investigated for designing a 50 W class tidal current turbine rotor blade. **Figure 3** shows the four selected hydrofoils (MNU26, NACA63421, DU91_W2_250, and DU93_W_210LM). Each hydrofoil has a different thickness ratio and hydrodynamic characteristics. Tidal current turbines must be capable of operating under sea water environment. It must be able to withstand the fatigue loading induced by the tidal current, water turbulence, temperature effects, and waves. A thick blade has a relatively high structural strength as compared to a thin blade. Therefore, in this study, hydrofoils with three different thicknesses were selected.

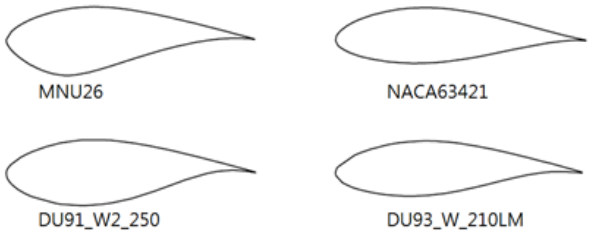


**Figure 3:** Selected hydrofoils for rotor blade

The MNU26 hydrofoil is a combined hydrofoil type that was used in a previous study **[7]**. The suction side of the DU91_W2_250 hydrofoil and the pressure side of the S814 hydrofoil were combined to produce the MNU26 hydrofoil.

Some points at the leading and trailing edges were also changed to provide a smooth curve. The MNU26 hydrofoil has a 26% thickness ratio that can be applied throughout the blade length, giving good structural strength. The NACA63421 **[8]** and DU93_W_210LM hydrofoils have a 21% thickness ratio, and the DU91_W2_250 hydrofoil has a 25% thickness ratio.

The hydrodynamic characteristics are very important in the selection of a high-performance hydrofoil. The performance of a turbine depends on three important parameters: the lift coefficient ($C_L$), lift to drag ratio ($C_L/C_D$), and Reynolds number. These three parameters vary with respect to the angle of attack ($AOA$) **[5]**. In this study, the design tidal current velocity is 1 m/s, and the Reynolds number is about $1 \times 10^5$.

**Figure 4** shows the CL and CL/CD curves at Reynolds number $1 \times 10^5$, which is calculated using X-Foil open source code **[9]**. The Reynolds number that is used in this study ($1 \times 10^5$) for the small tidal current turbine is relatively low compared to conventionally used Reynolds number (over $1 \times 10^6$) for tidal current turbines. Therefore, $C_L$ and $C_L/C_D$ curves have many variations for a low Reynolds number, and it is relatively difficult to obtain smooth hydrodynamic characteristics for $AOA$. Comparing the four hydrofoils, it was observed that MNU26 hydrofoil exhibited a higher $C_L$ and a relatively lower $C_L/C_D$ in contrast to the other three hydrofoils. The MNU26 hydrofoil showed different hydrodynamic characteristic compared to previous study **[7]** because of the different design parameters resulting from using a low Reynolds number.

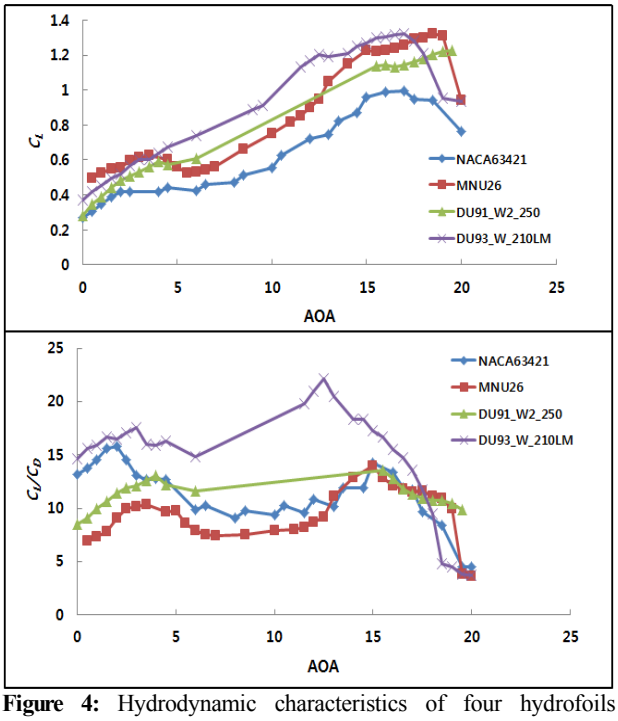


**Figure 4:** Hydrodynamic characteristics of four hydrofoils investigated at Reynolds number $1 \times 10^5$

## 3.2 Design of 50W class Rotor blade

**Table 2** presents the fundamental design parameters for the blades designed in this study. Using these design parameters and the four hydrofoils, four rotor blades were designed.

**Table 2**: Design parameters for blade design

| Design Parameters | Values |
|---|---|
| $P_{rated}$: Rated power | 50 W |
| $C_P$: Estimated power coefficient | 0.45 |
| $V_{rated}$: Rated current velocity | 1 m/s |
| $\rho$: Sea water density | 1024 kg/m$^3$ |
| $\lambda$: Tip speed ratio | 5 |
| $D$: Rotor diameter | 0.53 m |
| $N$: Blade number | 3 |
| $\omega$: Rotational speed | 180 min$^{-1}$ |
| $Re$: Reynolds number | $1 \times 10^5$ |

For the blade design, output power $P$ can be calculated with respect to current speed as in **equation (1)**. Since $P$ is directly proportional to the cube of the inflow current velocity, with the consideration of the rotation number of a generator in order to obtain the maximum output at tip speed ratio (TSR) λ = 5 as defined in **equation (2)**.

$$P = \frac{1}{2}\rho A V_\infty^3 \tag{1}$$

$$\lambda = \frac{R\omega}{V_\infty} \tag{2}$$

$$C_P = \frac{P_T}{\frac{1}{2}\rho A V_\infty^3} \tag{3}$$

Here, $\rho$ is the sea water density, $A$ is the swept area, $V_\infty$ is the inflow current velocity, and the blade radius $R$ is set as 0.265 m.

The power coefficient is given by **equation (3)**, where $P_T$ is the power from the turbine, which is the product of torque and angular velocity of the turbine rotor blade, and the denominator represents the power available, which is given by **equation (1)**.

**Figure 5** presents the twist angle, radius length, and chord length of the 50 W class optimized tidal current turbine rotor blade model designed in this study. When the blade was designed, each hydrofoil was used for the total length of the rotor blade.

The NACA63421 hydrofoil was used for the total length of the rotor blade. Circular profile sections are designed near the root section of the blade in order to strengthen the base of the

blade as shown in **Figure 6**. The other three blades were also designed by applying this method with each hydrofoil.

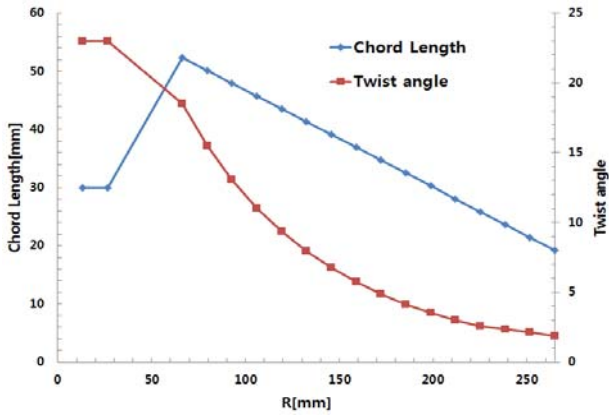


**Figure 5:** Twist angle, radial length and chord length of 50W class rotor blade model designed

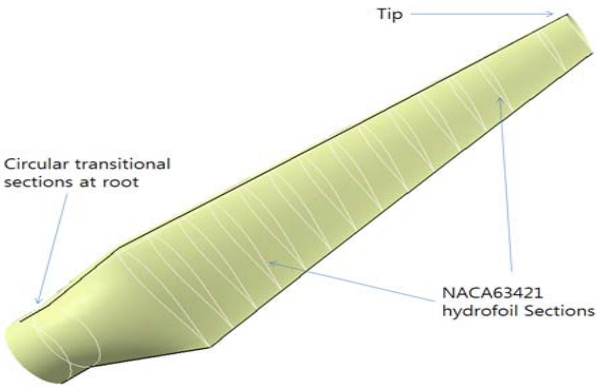


**Figure 6:** 50W class tidal current turbine rotor blade model designed using NACA63421 hydrofoil

## 4. Computational Analysis Method

### 4.1 Computational Grid

The computational grid of the 50 W class tidal current turbine is presented in **Figure 7**. Considering the computer capacity and calculation time, the model was meshed using ICEM CFD with a grid having a total of 6.5 million nodes. Hexahedral structural grids were used to increase the convergence of the calculation and its reliability.

The grid density of the blade surface is higher than that of the flow field surface because an O-Grid was used for the blade surface. A high grid density is required for the blade surface to achieve reliable CFD analysis results. Thus, the blade was refined to ensure that the $y^+$ value was less than 3. However, for efficient calculation time, the flow field is formed with a lower density with a gradual change in node distance. The steady state simulation was applied with a high resolution advection scheme until the simulation reached the required RMS residual stress value between $1 \times 10^{-5}$ and $1 \times 10^{-6}$.

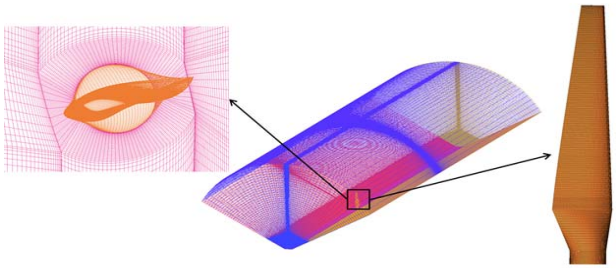

**Figure 7:** Numerical grid of total flow field for 50W class tidal current turbine rotor blade model

### 4.2 Calculation Conditions

The size of the total flow field is presented in **Figure 8**. The inlet and outlet surfaces were set at 8 and 12 times the blade radius, respectively, and the radial distance was set at 5 times the blade radius, as a large distance is required for a smooth transition of the flow.

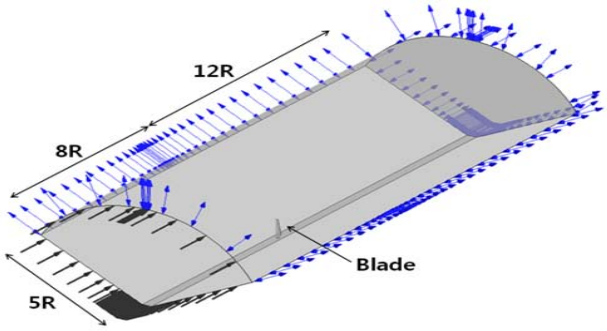


**Figure 8:** Size of total flow field of 50W class tidal current turbine rotor blade model

For numerical analysis of the 50 W class tidal current turbine rotor blade performance and fluid flow, ANSYS CFX **[10]**, a commercial CFD code, was used as a solver in this study. **Table 3** presents the calculation conditions used for the numerical analysis of the rotor blade. For the boundary conditions of the computational flow fields, the design current speed was set at the inlet, and the static pressure was set at the outlet. Sea water at 25 °C was used as the working fluid, and the steady state calculation was conducted. In order to confirm the performance and fluid flow for TSR values ranging between 3 and 8, the angular velocity was analyzed in the range of 11.32-30.19 rad/s. The shear stress transport (*SST*) turbulence model was utilized, which has been known to estimate both separation and vortex occurring on the wall of the blade.

**Table 3**: Calculation Condition for blade design

| Condition | Values |
|---|---|
| Inlet current speed | 1 m/s |
| Outlet static pressure | 0 Pa |
| Angular velocity | 11.32~30.19 rad/s |
| Turbulence model | SST |
| Surface of blade | No slip wall |

## 5. Calculation Results

### 5.1 Power Coefficient

**Equation (3)** is utilized in plotting the power coefficient curves for the four rotor blades investigated. The power coefficient curves are shown in **Figure 9**.

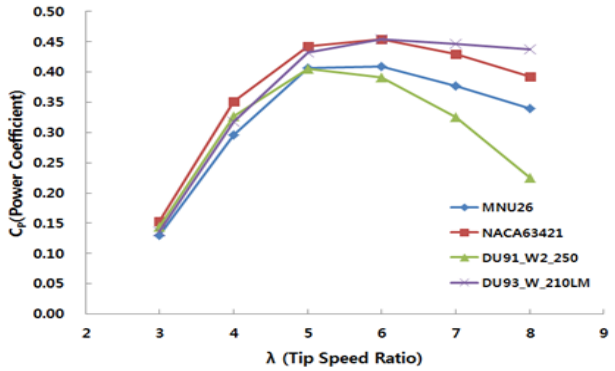


**Figure 9:** Power Coefficient Curve.

From the power coefficient curves, it is observed that blades having a hydrofoil with a relatively low thickness ratio showed a higher efficiency than those with a relatively higher thickness ratio. The maximum power coefficient of two turbines is about the same at around 0.45. NACA63421 and DU93_W_210LM blades had the maximum efficiency at TSR 6. NACA63421 blade had the maximum efficiency at a lower TSR compared to the other three turbines. In addition, DU93_W_210LM blade had the maximum efficiency at a higher TSR compared to the other three turbines. These results indicate that at a high current speed, the NACA63421 turbine performs better than the other three turbines. Moreover, the DU93_W_210LM turbine performs better than the other three turbines at a low current speed.

In this study, MNU26 blade shows a low $C_P$ value compared to the results of previous study **[5]**. This is because of the difference in the Reynolds number. The Reynolds number used in this study is 20 times different. The MNU26 hydrofoil shows different hydrodynamic characteristics because of a low Reynolds number whereas a higher Reynolds number was used in the previous study.

### 5.2 Pressure Distribution

The value of the pressure coefficient ($C_P$) surrounding the blade pressure surface and suction surface is compared quantitatively as shown in **Figure 10**, at 50%, 75%, 95% of the local radius for TSR 5. The area of the pressure coefficient curves denotes the pressure difference between the pressure surface and suction surface. A larger area indicates that the blade performance is good. As shown in **Figure 10**, X on the abscissa in the figures represents the chord length, which is the length from the leading edge to the trailing edge of the hydrofoil.

The maximum area of the pressure difference between the pressure and suction surfaces is observed at 75% of the local radius. By examining the pressure coefficient curves, it is observed that the maximum power is generated from approximately 75% of the blade radius to the tip. The area of the pressure difference between the pressure and suction surfaces at 75% of the local radius is observed at a relatively low thickness ratio of the blade, NACA63421 and DU93_W_210LM. However, the tidal current blade needs enough structural strength to withstand the extreme thrusts of the tidal current. Therefore, a small amount of power can be sacrificed for an optimum design. Further thinning of the blade would perhaps lead to fracture and a low lifespan.

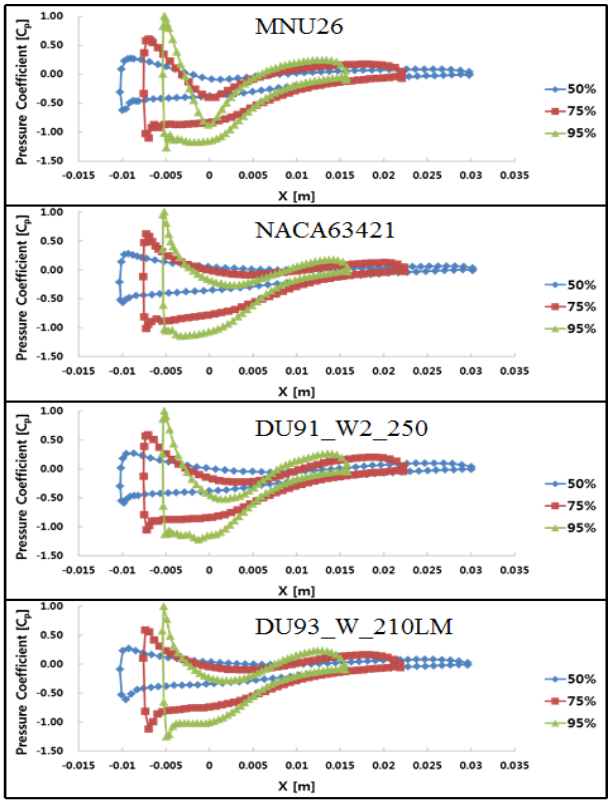


**Figure 10:** Pressure coefficient curves at 50%, 75%, 95% of the local radius

### 5.3 Streamline Distribution on the Blade Surface

**Figure 11** presents a clear streamline distribution on the blade surface for TSR 5, which is the design point of the turbine. From this figure, it can be observed that all the blades show secondary flow at the suction side surface. Moreover, the suction side surface shows the formation of radial flow. This radial flow creates an irregular flow on the blade surface and affects the hydrodynamic characteristics of the turbine by decreasing the output power and power coefficient.

However, pressure side surfaces show relatively uniform flow compared to the suction side surface. MNU26 and DU91_W2_250 hydrofoils showed the formation of secondary flow near the tip of the pressure side. This small difference in flow separation may be the reason for a lower power output.

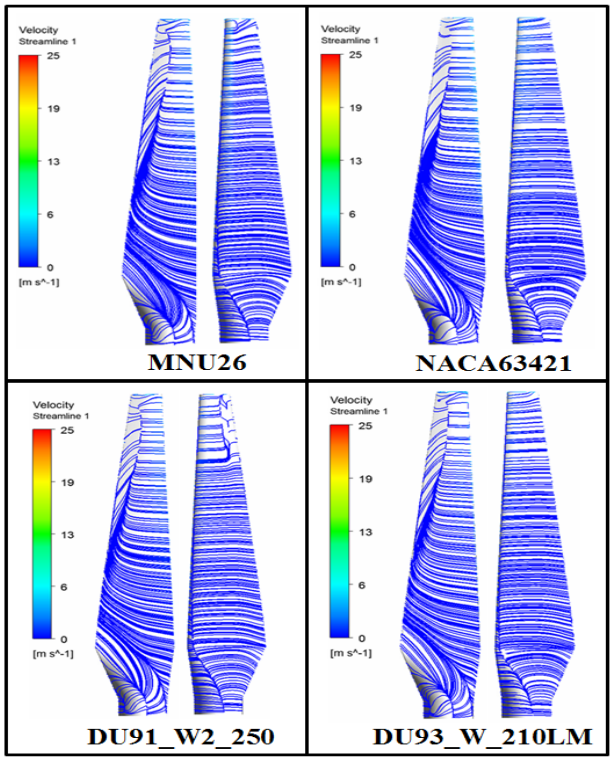


**Figure 11:** Streamlines on blade surface at TSR5

## 6. Conclusion

The following conclusions can be made from this study:

A 50 W class HATCT was designed using four hydrofoils with different hydrodynamic characteristic. It was confirmed that NACA63421 and DU93_W_210LM, which had a relatively low thickness ratio, had a higher efficiency than the MNU26 and DU91_W2_250 hydrofoil blades.

Among the four blades, the power coefficients of NACA63421 and DU93_W_210LM hydrofoil were higher than 0.4 from TSR 5-7, which is a significant advantage to generating more power.

Most of the power was generated at 75% of the blade length. By examining the pressure coefficient on the blade surface at 75% of the blade length, it was observed that the NACA63421 and DU93_W_210LM blades showed the maximum area of the pressure difference between the pressure and suction surface compared to the MNU26 and DU91_W2_250 blades. This difference may be the reason for the difference in power coefficient among the hydrofoils.

The streamlines showed a secondary flow at the suction surface of the four blades. However, the NACA63421 and DU93_W_210LM hydrofoils showed relatively good flow characteristics compared to the MNU26 and DU91_W2_250 hydrofoils at the pressure surface.

## Acknowledgement

This work was supported by the New and Renewable Energy of the Korea Institute of Energy Technology Evaluation and Planning (KETEP) grant funded by the Korea government Ministry of Trade, Industry and Energy (No. 20143030071350)

## References

[1] A. D. Hoang and C. J. Yang, "Performance comparison of 10kW scale horizontal axis tidal turbines," Journal of the Korean Society of Marine Engineering, vol. 38, no. 5, pp. 541-549, 2014.

[2] A. D. Hoang and C. J. Yang, "A fundamental study on velocity restoration for tidal farm," Journal of the Korean Society of Marine Engineering, vol. 37, no. 3, pp. 266-273, 2013.

[3] A. J. MacLeod, S. Barnes, K. G. Rados, and I. G. Bryden, "Wake effects in tidal current turbine farms," proceedings of the International Conference on Marine Renewable Energy-Conference, pp. 49-53, 2002.

[4] KEPCO in Brief, The Korea Electric Power Corporation, Korea, Available: www.kepco.co.kr, 2010-2011.

[5] T. Burton, D. Sharpe, N. Jenkins, and E. Bossanyi, Wind Energy Handbook, John Wiley & Sons, Ltd., 2001.

[6] D. S. Byun, D. E. Hart, and W.-J. Jeong, "Tidal current energy resources off the south and west coasts of Korea: Preliminary observation-derived estimates," Energies, vol. 6, no. 2, pp. 566-578, 2013.

[7] M. S. Patrick and Y. D. Choi, "Shape design and numerical analysis on a 1MW tidal current turbine for the south-western coast of Korea," Renewable Energy,

vol. 68, pp. 485-493, 2014.

[8] N. J. Lee, I. C. Kim, C. G. Kim, B. S. Hyun, and Y. H. Lee, "Performance study on a counter-rotating tidal current turbine by CFD and model experimentation," Renewable Energy, vol. 79, pp. 122-126, 2015.

[9] MIT Aero & Astro, http://web.mit.edu/drela/Public/web/xfoil/, Accessed March 11, 2015.

[10] ANSYS Inc, "ANSYS CFX Documentation," Ver. 13. http://www.ansys.com, Accessed November 10, 2013.